

UC Riverside

UC Riverside Previously Published Works

Title

Supramolecular Fullerene-Porphyrin Chemistry. Fullerene Complexation by Metalated “Jaws Porphyrin” Hosts

Permalink

<https://escholarship.org/uc/item/814160w1>

Journal

Journal of the American Chemical Society, 124(23)

ISSN

0002-7863

Authors

Sun, Dayong
Tham, Fook S
Reed, Christopher A
[et al.](#)

Publication Date

2002-06-01

DOI

10.1021/ja017555u

Peer reviewed

Supramolecular Fullerene-Porphyrin Chemistry. Fullerene Complexation by Metalated "Jaws Porphyrin" Hosts

Dayong Sun,[†] Fook S. Tham,[†] Christopher A. Reed,^{*,†} Leila Chaker,[‡] and Peter D. W. Boyd^{*,‡}

Contribution from the Departments of Chemistry, University of California, Riverside, California 92521-0403, and The University of Auckland, Private Bag, Auckland, New Zealand

Received November 15, 2001

Abstract: Porphyrins and fullerenes are spontaneously attracted to each other. This new supramolecular recognition element is explored in discrete, soluble, coordinatively linked porphyrin and metalloporphyrin dimers. Jawlike clefts in these bis-porphyrins are effective hosts for fullerene guests. X-ray structures of the Cu complex with C₆₀ and free-base complexes with C₇₀ and a pyrrolidine-derivatized C₆₀ have been obtained. The electron-rich 6:6 ring-juncture bonds of C₆₀ show unusually close approach to the porphyrin or metalloporphyrin plane. Binding constants in toluene solution increase in the order Fe(II) < Pd(II) < Zn(II) < Mn(II) < Co(II) < Cu(II) < 2H and span the range 490–5200 M⁻¹. Unexpectedly, the free-base porphyrin binds C₆₀ more strongly than the metalated porphyrins. This is ascribed to electrostatic forces, enhancing the largely van der Waals forces of the π - π interaction. The ordering with metals is ascribed to a subtle interplay of solvation and weak interaction forces. Conflicting opinions on the relative importance of van der Waals forces, charge transfer, electrostatic attraction, and coordinate bonding are addressed. The supramolecular design principles arising from these studies have potential applications in the preparation of photophysical devices, molecular magnets, molecular conductors, and porous metal-organic frameworks.

Introduction

As discrete molecules, the chemistry of fullerenes has been explored in three identifiable phases. Early investigations emphasized their synthesis and redox chemistry, and understanding the new type of bonding presented by their curved π surfaces.¹ Organic functionalization chemistry followed.^{2–5} Now, the supramolecular chemistry of fullerenes is attracting attention.^{6,7}

This paper concerns a newly recognized supramolecular recognition element, the attraction of the curved π surface of a fullerene to the center of the flat π surface of a porphyrin or metalloporphyrin. In contrast to the traditional paradigm, it is not necessary to match a concave host with a convex guest. The interaction has attracted attention from a fundamental point of view,⁸ and there are potential applications in fullerene-

porphyrin light-harvesting devices,^{9–11} molecular conductors or magnets,^{12–14} medicine,¹⁵ and porous metal-organic frameworks.¹⁶

The close association of a fullerene and a porphyrin was first recognized in the solid-state porphyrin-fullerene assembly of a covalent fullerene-porphyrin conjugate.¹⁷ In the crystal structure of this species, the 2.75 Å approach of a fullerene carbon atom to center of a porphyrin plane was notably shorter than separations of familiar π - π interactions. Graphite and typical arene/arene separations are in the range 3.3–3.5 Å. Interfacial porphyrin/porphyrin separations are >3.2 Å, fullerene/arene approaches lie in the range 3.0–3.5 Å, and fullerene/fullerene separations are typically ca. 3.2 Å.¹⁷ Two conclusions were drawn.

First, the close approach was proposed to reflect an attractive, structure-defining π - π interaction. The frequency with which it has appeared in subsequent research supports this notion.

* To whom correspondence should be addressed. E-mail: chris.reed@ucr.edu and pdw.boyd@auckland.ac.nz.

[†] University of California, Riverside.

[‡] The University of Auckland.

- (1) *Accounts of Chemical Research*; American Chemical Society: Washington, DC, March, 1992; Vol. 25.
- (2) Taylor, R.; Walton, D. R. M. *Nature* **1993**, 363, 685–693.
- (3) Hirsch, A. *The Chemistry of the Fullerenes*; Georg Thieme Verlag Stuttgart: New York, 1994.
- (4) Diederich, F.; Thilgen, C. *Science* **1996**, 271, 317–323.
- (5) Taylor, R. *Lecture Notes in Fullerene Chemistry*; Imperial College Press: London, 1999.
- (6) Constable, E. C. *Angew. Chem., Int. Ed. Engl.* **1994**, 33, 2269–2271.
- (7) Diederich, F.; Gómez-López, M. *Chem. Soc. Rev.* **1999**, 28, 263–277.
- (8) Boyd, P. D. W.; Hodgson, M. C.; Chaker, L.; Rickard, C. E. F.; Oliver, A. G.; Brothers, P. J.; Bolskar, R.; Tham, F. S.; Reed, C. A. *J. Am. Chem. Soc.* **1999**, 121, 10487–10495.
- (9) Guldi, D. M. *Chem. Commun.* **2000**, 321–327.
- (10) Segura, J. L.; Martin, N. *Chem. Soc. Rev.* **2000**, 29, 13–25.
- (11) Armaroli, N.; Marconi, G.; Echegoyen, L.; Bourgeois, J.-P.; Diederich, F. *Chem.-Eur. J.* **2000**, 6, 1629.
- (12) Kahn, O. *Molecular Magnetism*; VCH: New York, 1993.
- (13) Eichhorn, D. M.; Yang, S.; Jarrell, W.; Baumann, T. F.; Beall, L. S.; White, A. J. P.; Williams, D. J.; Barrett, A. G. M.; Hoffman, B. M. *J. Chem. Soc., Chem. Commun.* **1995**, 1703–1704.
- (14) Konarev, D. V.; Lyubovskaya, R. N. *Usp. Khim.* **1999**, 68, 23–44.
- (15) Da Ros, T.; Prato, M. *Chem. Commun.* **1999**, 663–669.
- (16) Sun, D.; Tham, F. S.; Reed, C. A.; Boyd, P. D. W. *Proc. Natl. Acad. Sci. U.S.A.* **2002**, 99, 5088–5092.
- (17) Sun, Y.; Drovetskaya, T.; Bolskar, R. D.; Bau, R.; Boyd, P. D. W.; Reed, C. A. *J. Org. Chem.* **1997**, 62, 3642–3649.

Reports soon appeared of cocrystallates of fullerenes with octaethylporphyrin (H₂OEP) and metallooctaethylporphyrins,¹⁸ and with tetraphenylporphyrins⁸ (H₂TPP). More examples followed,^{19–25} and fullerenes are attracted to other flat π surfaces.^{13,26–28} The curved to flat π – π attraction has been analyzed by molecular mechanics modeling and shown to be largely the result of van der Waals dispersion forces.⁸ Further, the interaction is not merely a feature of solid-state cocrystallizations; it persists in solution.⁸ This has been shown elegantly with covalently linked bis-porphyrin hosts that take up fullerene guests having binding constants up to $7 \times 10^5 \text{ M}^{-1}$ in toluene.^{29–31} These values can exceed those of traditional concave hosts such as calixarenes,³² cyclotrimeratralenes,^{33,34} and resorcarenes,³⁵ showing that the matching of convex and concave surfaces is not a requirement for strong supramolecular π – π complexation.

Second, it was proposed that the fullerene-porphyrin π – π interaction involved some degree of electrostatic attraction or charge transfer.¹⁷ In particular, it was proposed that the electron-rich “double bond” at the 6:6 ring juncture of C₆₀ or C₇₀ was attracted to the protic center of the free-base porphyrin. This proposal was counter to the prevailing notion of fullerenes acting as electron acceptors. Indeed, the electron-accepting ability of fullerenes is probably their most characteristic chemical property.³⁶ This is illustrated in metalloporphyrin chemistry by the reaction of Cr^{II}(TPP) with C₆₀ in tetrahydrofuran to give the Cr(III) fulleride salt [Cr(THF)₂(TPP)][C₆₀]³⁷ or the reaction of Sn^{II}(TPP) with C₆₀ in the presence of *N*-methylimidazole to give [Sn^{IV}(N-MeIm)₂(TPP)][C₆₀]₂.³⁷ However, because of the delocalized nature of the C₆₀ LUMO, fullerene electronegativity is fundamentally a global property, whereas the proposed

fullerene/porphyrin interaction is a more local one. One approach to address the charge transfer question is to study metalated porphyrin hosts and determine how the fullerene responds as a function of metal. The roles of hard, first row transition metals in metalloporphyrins can be expected to be quite different from soft metals in phosphine complexes such as Ni(C₆₀)(PET₃)₂³⁸ or IrCl(C₆₀)(CO)(PPh₃)₂³⁹ because hard metals have little or no opportunity to engage in π back-bonding.

We have reported that the complex of Fe(TPP)⁺ with C₆₀ is green rather than purple, the expected color of the combined unperturbed chromophores.¹⁹ This implies charge transfer via coordinate bonding. The Fe atom is slightly out-of-plane toward the C₆₀ indicating the presence of a weak axial coordinate bond with at least some degree of covalence. The orbitals involved were identified by density functional theory in closely related complexes of Fe(TPP)⁺ with η^2 -bonded arenes.¹⁹ Because the Fe(III) center is cationic and its d_{z²} orbital is only half occupied, it would be difficult to argue that the direction of charge transfer is not with the fullerene as the donor. On the other hand, many fullerene-M(OEP) structures have been interpreted as indicating no covalent interaction,¹⁸ and some structures apparently have the less electron-rich 5:6 (rather than a 6:6) ring-juncture bond closest to the metalloporphyrin.^{20,22} Another recent study concludes that these molecular complexes have no charge transfer in the ground state.²³ Evidence that C₆₀ has sufficient ligand field strength to cause a high to low spin-state change in Mn(TPP) has also been forwarded,²³ but this contradicts field strength deductions based on other Mn(TPP) chemistry⁴⁰ and isoelectronic Fe(III) chemistry.¹⁹ A recent communication reports that binding constants for C₆₀ increase as a function of the metal in a bis-porphyrin host in the order Ag(I) < Ni(II) < Cu(II) < Zn(II) < free base < Co(II) < Rh(III).⁴¹ With the exception of rhodium(III), the differences are quite small, and the ordering has not been interpreted. The ordering changes slightly with C₇₀.⁴¹ Synthesizing a coherent understanding of these sometimes conflicting observations is the goal of this paper. We address the problem by studying the complexation of C₆₀ and C₇₀ guests in metalated “jaws porphyrin” hosts.

Results and Discussion

Design and Synthesis of Jaws Porphyrin. The design of “jaws” porphyrins evolved from an interplay of molecular modeling and experiment. The basic bis-porphyrin motif was cut from the common zigzag structural arrangement seen in self-assembling tetraphenylporphyrin/fullerene cocrystallates.⁸ Various linkers such as those illustrated in Figure 1 were used to construct bis-porphyrins as fullerene binding hosts maintaining this motif. The design criteria, based on cocrystallate structures, allowed for a porphyrin–porphyrin intercenter distance of 11.5–12 Å with interplanar porphyrin angles of 40–60°. Host–guest complexes with C₆₀ were constructed and subjected to geometry optimization with molecular mechanics calculations. In each case, the gas-phase binding enthalpy was determined together with the geometry of the free bis-porphyrin host. It became clear

- (18) Olmstead, M. M.; Costa, D. A.; Maitra, K.; Noll, B. C.; Phillips, S. L.; Van Calcar, P. M.; Balch, A. L. *J. Am. Chem. Soc.* **1999**, *121*, 7090–7097.
- (19) Evans, D. R.; Fackler, N. L. P.; Xie, Z.; Rickard, C. E. F.; Boyd, P. D. W.; Reed, C. A. *J. Am. Chem. Soc.* **1999**, *121*, 8466–8474.
- (20) Ishii, T.; Aizawa, N.; Yamashita, M.; Matsuzaka, H.; Kodama, T.; Kikuchi, K.; Ikemoto, I.; Iwasa, Y. *J. Chem. Soc., Dalton Trans.* **2000**, 4407–4412.
- (21) Olmstead, M. M.; de Bettencourt-Dias, A.; Duchamp, J. C.; Stevenson, S.; Dorn, H. C.; Balch, A. L. *J. Am. Chem. Soc.* **2000**, *122*, 12220–12226.
- (22) Ishii, T.; Aizawa, N.; Kanehama, R.; Yamashita, M.; Matsuzaka, H.; Kodama, T.; Kikuchi, K.; Ikemoto, I. *Inorg. Chim. Acta* **2001**, *317*, 81–90.
- (23) Konarev, D. V.; Neretin, I. S.; Slovokhotov, Y. L.; Yudanov, E. I.; Drichko, N. V.; Shul'ga, Y. M.; Tarasov, B. P.; Gumanov, K. L.; Batsanov, A. S.; Howard, J. A. K.; Lyubovskaya, R. N. *Chem.-Eur. J.* **2001**, *7*, 2605–2616.
- (24) Ishii, T.; Kanehama, R.; Aizawa, N.; Masahiro, Y.; Matsuzaka, H.; K-i., S.; Miyasaka, H.; Kodama, T.; Kikuchi, K.; Ikemoto, I.; Tanaka, H.; Marumoto, K.; Kuroda, S.-I. *J. Chem. Soc., Dalton Trans.* **2001**, 2975–2980.
- (25) Ishi-i, T.; Iguchi, R.; Snip, E.; Ikeda, M.; Shinkai, S. *Langmuir* **2001**, *17*, 5825–5833.
- (26) Andrews, P. C.; Atwood, J. L.; Barbour, L. J.; Nichols, P. J.; Raston, C. L. *Chem.-Eur. J.* **1998**, *4*, 1384–1387.
- (27) Balch, A. L.; Olmstead, M. M. *Coord. Chem. Rev.* **1999**, *185–186*, 601–617.
- (28) Hochmuth, D. H.; Michel, S. L. J.; White, A. J. P.; Williams, D. J.; Barrett, A. G. M.; Hoffman, B. M. *Eur. J. Inorg. Chem.* **2000**, 593–596.
- (29) Tashiro, K.; Aida, T.; Zheng, J.-Y.; Kinbara, K.; Saigo, K.; Sakamoto, S.; Yamaguchi, K. *J. Am. Chem. Soc.* **1999**, *121*, 9477–9478.
- (30) Sun, D.; Tham, F. S.; Reed, C. A.; Chaker, L.; Burgess, M.; Boyd, P. D. W. *J. Am. Chem. Soc.* **2000**, *122*, 10704–10705.
- (31) Nishioka, T.; Tashiro, K.; Aida, T.; Zheng, J.-Y.; Kinbara, K.; Saigo, K.; Sakamoto, S.; Yamaguchi, K. *Macromolecules* **2000**, *33*, 9182–9184.
- (32) Atwood, J. L.; Koutsantonis, G. A.; Raston, C. L. *Nature* **1994**, *368*, 229–232.
- (33) Steed, J. W.; Junk, P. C.; Atwood, J. L.; Barnes, M. J.; Raston, C. L.; Burkhalter, R. S. *J. Am. Chem. Soc.* **1994**, *116*, 10346–10347.
- (34) Matsubara, H.; Hasegawa, A.; Shiwa, K.; Asano, K.; Uno, M.; Takahashi, S.; Yamamoto, K. *Chem. Lett.* **1998**, 923–924.
- (35) Fox, O. D.; Drew, M. G. B.; Wilkinson, E. J. S.; Beer, P. D. *Chem. Commun.* **2000**, 391–392 and references therein.
- (36) Reed, C. A.; Bolskar, R. D. *Chem. Rev.* **2000**, *100*, 1075–1119.
- (37) Stinchcombe, J.; Pénicaud, A.; Bhyrappa, P.; Boyd, P. D. W.; Reed, C. A. *J. Am. Chem. Soc.* **1993**, *115*, 5212–5217.

- (38) Fagan, P. J.; Calabrese, J. C.; Malone, B. *Acc. Chem. Res.* **1992**, *25*, 134–142.
- (39) Balch, A. L.; Olmstead, M. M. *Chem. Rev.* **1998**, *98*, 2123–2166.
- (40) Kirner, J. F.; Reed, C. A.; Scheidt, W. R. *J. Am. Chem. Soc.* **1977**, *99*, 2557–2563.
- (41) Zheng, J.-Y.; Tashiro, K.; Hirabayashi, Y.; Kinbara, K.; Saigo, K.; Aida, T.; Sakamoto, S.; Yamaguchi, K. *Angew. Chem., Int. Ed.* **2001**, *40*, 1858–1861.

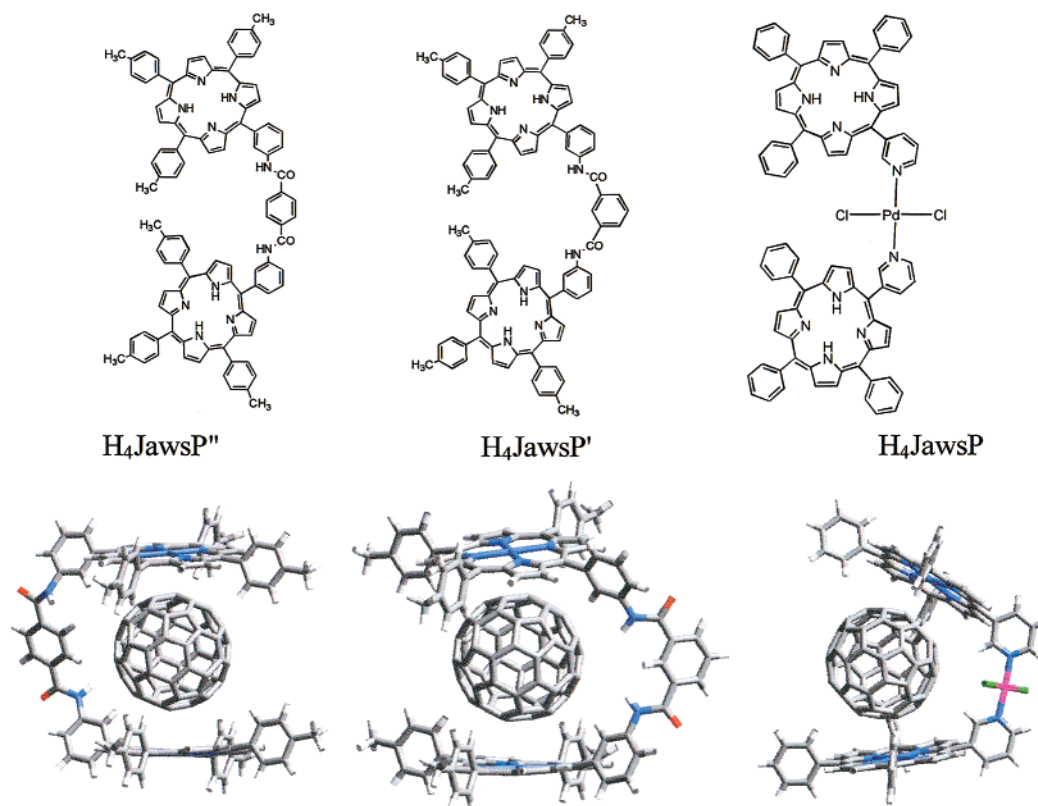


Figure 1. Representative “jaws porphyrin” hosts and the calculated structures of their C_{60} host–guest complexes. From left to right: H_4JawsP'' , H_4JawsP' , and H_4JawsP .

that some hosts were significantly strained in the host–guest complexes. Of the three shown in Figure 1, only H_4JawsP and H_4JawsP' gave plausible binding energies and unstrained structures.

Soft ionization MALDI mass spectrometry turns out to be an excellent rapid qualitative assay for fullerene binding to porphyrin hosts. Using a dithronol matrix, 1:1 fullerene:bisporphyrin complexes give exact mass peaks corresponding to both the supramolecular complexes and their constituent parts, and the abundance ratios of complexes relative to constituent parts roughly correlate with binding constants derived in solution. By contrast, cocrystallized monomeric porphyrin/fullerene complexes retain no complexation when gas-phase ions are produced under comparable conditions. Of the three examples illustrated in Figure 1, H_4JawsP'' showed little evidence of binding to C_{60} , H_4JawsP' showed some interaction, and H_4JawsP (right side of Figure 1) was the best.

These results are consistent with 1H NMR results in solution. Upfield shifts of the central N–H proton at -2.3 ppm indicate fullerene complexation because of the ring current effect of the fullerene on the porphyrin. The larger the upfield shift is, the greater the binding.⁸ When equimolar amounts of the bisporphyrins and C_{60} are mixed in toluene- d_8 /chloroform- d_3 , the shifts for 10^{-4} M solutions were 0.01, 0.04, and 0.11 ppm for H_4JawsP'' to H_4JawsP' to H_4JawsP , respectively. The corresponding gas-phase binding energies from molecular mechanics were estimated as 32.0, 44.9, and 57.4 kcal mol $^{-1}$.

MALDI also appears to be a useful indicator of selectivity. For example, when a mixture of C_{60} and smaller amounts of higher fullerenes (including C_{70} , C_{76} , C_{78} , and C_{84}) was treated with somewhat less than 1 equiv of Cu_2JawsP , the MALDI

spectrum showed *more* C_{84} complex than C_{60} complex (Figures S1 and S2). This indicates that C_{84} binds to the porphyrin host more strongly than does C_{60} , an observation that is consistent with the displacement of C_{60} by C_{70} from the host in solution experiments.³⁰ Greater van der Waals interactions are possible with higher fullerenes. The result with a gadolinium endohedral fullerene is even more interesting. A minor peak due to $Gd@C_{82}$ in the spectrum of a mixture with C_{60} , C_{70} , C_{76} , C_{78} , and C_{84} becomes the major peak of 1:1 complexes when treated with H_4JawsP (Figures S3 and S4). This suggests that endohedral fullerenes bind more strongly to porphyrin hosts than do empty fullerenes, consistent with the high selectivity that porphyrin-appended silica stationary phases show in fullerene and endohedral fullerene chromatography.⁴² Stronger binding of endohedral fullerenes relative to same-size empty fullerenes suggests an increased electrostatic component to the porphyrin–fullerene interaction. The exterior surface of endohedral fullerenes, derived from electropositive metals such as gadolinium, must have fulleride character. This would enhance attraction to the positive center of the porphyrin and help to explain why metallocporphyrins have been successful in crystallizing interesting endohedral fullerenes.²¹

The $PdCl_2$ linkage to the meta-pyridyl functionality in H_4JawsP optimizes fullerene fit and preorganization. The meta-*tert*-butyl substituents were added for good solubility in low dielectric organic solvents. Divalent metals (Pd, Zn, Cu, Co, Fe, and Mn) were readily inserted into H_4JawsP via standard methods, except that Ni(II) competition with Pd in the linkage thwarted the synthesis of $Ni_2(JawsP)$. Host/guest complexation

(42) Xiao, J.; Savina, M. R.; Martin, G. B.; Francis, A. H.; Meyerhoff, M. E. *J. Am. Chem. Soc.* **1994**, *116*, 9341–9342.

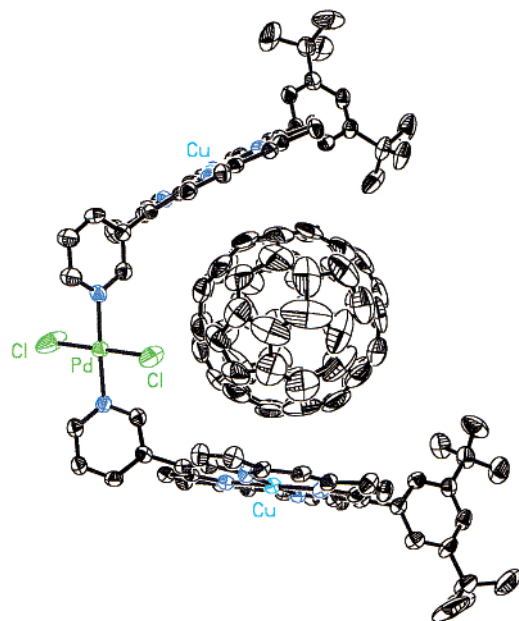


Figure 2. Perspective drawing of the crystal structure of $\text{Cu}_2(\text{JawsP})\cdot\text{C}_{60}$. A pair of *trans* 3,5-di-*tert*-butylphenyl substituents on each porphyrin have been omitted for clarity. Thermal ellipsoids are shown at 50% level.

with fullerenes was typically investigated in toluene solution. Arene solvents are known to solvate fullerenes and porphyrins well,⁴³ so the choice of toluene sets up a real competition. The binding constants are not artificially exaggerated by solvent/solute incompatibility.

X-ray Structures of Fullerene Complexes. Crystals of jaws porphyrin/fullerene complexes suitable for X-ray structure determination were obtained for four derivatives: (a) C_{60} with a mixture of Pd(II) and free-base porphyrin, $\text{Pd}_{1.5}\text{H}(\text{JawsP})\cdot\text{C}_{60}$, reported earlier,³⁰ (b) C_{60} with the copper(II) metalated porphyrin, $\text{Cu}_2(\text{JawsP})\cdot\text{C}_{60}$, (c) a common functionalized fullerene, *N*-methylpyrrolidino- C_{60} , with free-base porphyrin, and (d) C_{70} with free-base porphyrin, $\text{H}_4(\text{JawsP})\cdot 2\text{C}_{70}$. As is common in fullerene crystallography, disorder diminishes the detailed information available from these structures, but the essential structural features can be deduced. All show the now familiar attraction of the fullerene to the center of the porphyrin or metalloporphyrin. In all three C_{60} structures, it is a 6:6 rather than the 6:5 ring-juncture bond that most closely approaches the porphyrin or metalloporphyrin.

Three features of the $\text{Cu}_2(\text{JawsP})\cdot\text{C}_{60}$ structure are worthy of comment. First, the 24-atom porphyrin core is slightly domed and ruffled. The doming may be to wrap the fullerene more effectively (see Figure 2) and is presumably the result of maximizing attractive van der Waals contact. Ruffling of metalloporphyrins is related to the size of the central metal, small metals such as Cu(II) typically leading to S_4 ruffling.⁴⁴ A similar warping of macrocycles is observed in fullerene complexes with metalloporphyrazines²⁸ and other metallo-tetraphenylporphyrins.²³

Second, the $\text{Cu}\cdots\text{C}$ distances are relatively long (2.83 and 3.06 Å to a 6:6 ring juncture), and the copper atom is not drawn out of the porphyrin plane toward the fullerene. In fact, the Cu

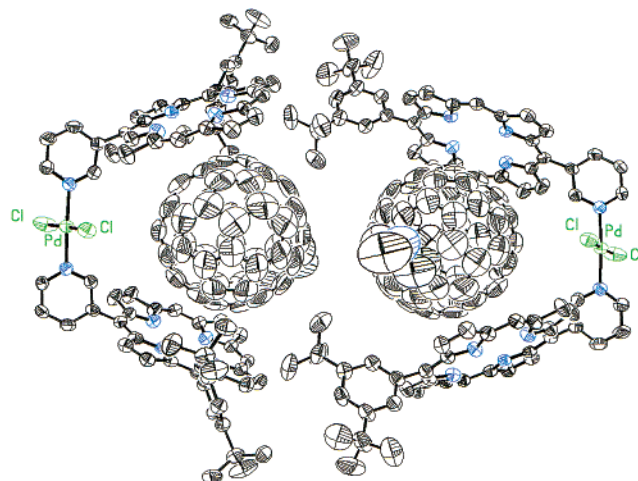


Figure 3. Perspective drawing of the crystal structure of the complex of *N*-methylpyrrolidine-functionalized C_{60} with free-base jaws porphyrin showing the pairing common to all C_{60} structures.

atom protrudes out of the porphyrin plane in the opposite direction (0.024 Å from the mean N_4 plane) because of the overall doming and asymmetric warping of the porphyrin. As in the Pd analogue where the closest approach is 2.85 Å,³⁰ this indicates a relatively insignificant role for coordinate bonding. For comparison, the closest $\text{Fe}\cdots\text{C}$ distance in $[\text{Fe}(\text{C}_{60})(\text{TPP})]^+$ is 2.63 Å, and the Fe atom is slightly out-of-plane toward the fullerene.¹⁹

Third, inspection of the crystal packing reveals a fullerene–fullerene van der Waals contact. The complexes occur in pairs allowing van der Waals contact of the fullerenes. Interestingly, the 6:6 ring-juncture bonds are in perfect alignment, as though set up for a $[2 + 2]$ cycloaddition reaction. The $\text{C}\cdots\text{C}$ separation is 3.29 Å. Even when the fullerene is derivatized with *N*-methylpyrrolidine, the same alignment is observed in pairs of complexes (see Figure 3). The $\text{C}\cdots\text{C}$ separation is almost identical at 3.30 Å. In fact, the pairing feature is found in all three C_{60} jaws porphyrin structures. It suggested to us that a 2:1 bis-porphyrin:fullerene complex might form with a dimeric fullerene such as C_{120} or C_{120}O . However, using mass spectrometry as mentioned earlier, we found evidence only for the 1:1 complex with pure C_{120}O , so crystallization studies were not pursued. The carbon atom closest to the porphyrin center in the *N*-methylpyrrolidine structure (Figure 3) is three atoms removed from the functionality. Mulliken population analysis in a semiempirical MO calculation⁴⁵ shows this to be the most negative atom that is sterically accessible to the porphyrin plane, indicating an electrostatic component to the orientation of the fullerene. This carbon atom (C15F) is 2.76 Å from the 4N mean plane.

Although fullerene/fullerene $\text{C}\cdots\text{C}$ contacts at ca. 3.3 Å appear in several crystal structures⁸ and can be significant,⁴⁶ they are clearly subservient to porphyrin–fullerene interactions. All fullerene–porphyrin cocrystallates have fullerene–porphyrin interactions, but not all have fullerene–fullerene contacts.

The $\text{H}_4(\text{JawsP})\cdot 2\text{C}_{70}$ structure differs from the other structures in that an “extra” fullerene is accommodated in the lattice. As shown in Figure 4, this fullerene acquires the familiar porphyrin–fullerene interaction by association with the “outside”

(43) Noviadri, I.; Bolskar, R. D.; Lay, P. A.; Reed, C. A. *J. Phys. Chem. B* **1997**, *101*, 6350–6358.

(44) Scheidt, W. R.; Lee, Y. J. *Struct. Bonding* **1987**, *64*, 1–70.

(45) Stewart, J. J. P. *J. Comput. Chem.* **1989**, *10*, 209–220.

(46) Barbour, L. J.; Orr, G. W.; Atwood, J. L. *Chem. Commun.* **1998**, 1901.

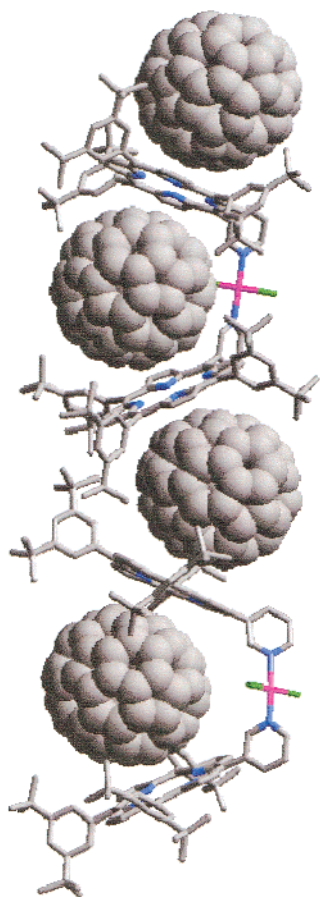


Figure 4. Perspective drawing of the crystal structure of $H_4(\text{JawsP}) \cdot 2C_{70}$ showing C_{70} complexed within, and cocrystallized outside, the free-base jaws porphyrin.

of the jaws porphyrin. In this way, it is reminiscent of earlier cocrystallates.⁸ The C_{70} that is complexed within the jaws of the porphyrin is bound “side-on” rather than “end-on”, confirming structural deductions based on ^{13}C NMR.³⁰ This presumably maximizes van der Waals attraction since the flatter equatorial regions of C_{70} have more contact with the porphyrin than the more highly curved polar regions.⁸

UV–Vis Spectroscopy. Small red shifts of the Soret bands of porphyrins and metalloporphyrins (up to 7 nm) have been noted upon complexation of fullerenes.^{23,29} Shifts in the lower energy α, β bands are smaller or nonexistent. Because of the high dilution required to keep porphyrin absorptivities on-scale in a spectrometer, it is difficult to gain the complete measure of these small shifts in solution. However, when 10^{-5} M toluene solutions of the jaws porphyrin derivatives are treated with high concentrations of C_{60} , small shifts are sometimes observed. For the free base and the Zn complex, the Soret band is red-shifted by 2–3 nm upon complexation. For Cu and Co, the change is insignificant. For Pd, there is a 1 nm blue shift. Red shifting may reflect the donation of electron density from the axial ligand to the porphyrin ring, lowering the energy of the π to π^* transition,^{47,48} consistent with the fullerene acting as a weak donor. However, the shifts are too small for definitive interpretation.

(47) Gouterman, M.; Schwarz, F. P.; Smith, P. D.; Dolphin, D. *J. Chem. Phys.* **1973**, *59*, 676.

(48) Nappa, M.; Valentine, J. S. *J. Am. Chem. Soc.* **1978**, *100*, 5075–5080.

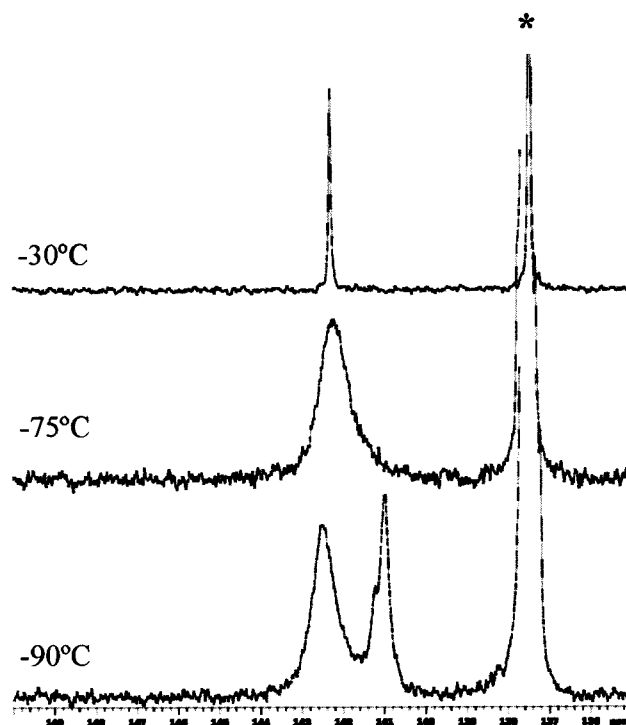


Figure 5. Variable temperature ^{13}C NMR spectrum of a 1:3 mixture of $\text{Pd}_2(\text{JawsP})$ and C_{60} . The asterisk marks solvent peaks (toluene).

Table 1. C_{60} ^{13}C NMR Data on $M_2(\text{JawsP}) \cdot C_{60}$ in Toluene

M	δ at -90°C (ppm)	coalescence temp ($^\circ\text{C}$)	binding constant (M^{-1})
Pd(II)	140.8	−75	815 ± 120
Zn(II)	140.2	−60	1945 ± 750
2H	140.0	−50	5200 ± 120
Cu(II)	140.5 (br)	−45	4860 ± 250
Mn(II)	<i>a</i>	−15	2760 ± 120
Fe(II)	190 (br)	−45	490 ± 15
Co(II)	192 (br)	25	2975 ± 120

^a Extremely broad.

NMR Spectroscopy. Variable temperature NMR spectroscopy is a powerful technique for assessing the thermodynamic and kinetic aspects of fullerene complexation.³⁰ In the present work, we use NMR spectroscopy to determine the relative binding constants of C_{60} to $M_2(\text{JawsP})$ as a function of metal, with the added complication that paramagnetic metals introduce chemical shifts that are intrinsically temperature-dependent. Toluene- d_8 was used as solvent, and ^{13}C -enriched C_{60} (10–15%) was used to enhance signal quality.

Figure 5 shows the variable temperature ^{13}C NMR spectrum of a 1:3 mixture of the palladium(II) metalated porphyrin, $\text{Pd}_2(\text{JawsP})$, and C_{60} . At -90°C , two fullerene peaks are seen at 141.0 and 142.6 ppm, assigned to complexed and uncomplexed C_{60} , respectively. At this temperature, the complex must be in the slow exchange regime. Upon warming, coalescence of these two signals is seen at -75°C . At -30°C , the sharpness of the single peak at 142.5 indicates rapid exchange between complexed and uncomplexed fullerene. The chemical shift reflects a weighted average, plus the minor effects of temperature on the intrinsic chemical shifts. As summarized in Table 1, similar results are obtained with the zinc-metalated porphyrin with respect to both chemical shift and coalescence temperature. The observations are completely reversible and are similar to

those with free-base porphyrin whose chemical shift in the slow exchange limit is 140.0 ppm.³⁰ Both the Pd(II) and the Zn(II) metalloporphyrins and the free-base porphyrin produce upfield chemical shifts on C₆₀, consistent with a ring current effect from a diamagnetic π system of the porphyrin. This is confirmed in the ¹³C CPMAS NMR spectra of cocrystallates such as H₂TPP·C₆₀·3toluene which shows a 3.2 ppm upfield shift of the C₆₀ signal relative to free C₆₀ powder. In both cases, the room-temperature peak is sharp, indicating rapid tumbling of C₆₀ on the NMR time scale.⁴⁹

In the solution measurements, the coalescence temperature of the free-base complex (−50 °C) is higher than that of the zinc complex (−60 °C) and palladium (−75 °C), indicating that C₆₀ binds more strongly to H₄JawsP than the Pd or Zn porphyrins in the order Pd < Zn < 2H. This conclusion can be drawn because the chemical shift differences between bound and unbound C₆₀ in each case are of similar magnitude. Competition experiments confirm this conclusion. When C₆₀ is titrated into a 2:3 mixture of H₄JawsP and Pd₂(JawsP), peaks in the ¹H NMR spectrum of the free-base porphyrin respond immediately, whereas those of the palladium-metalated porphyrin respond only after ca. 1 equiv of C₆₀ has been added. For example, in a mixture containing H₄JawsP, Pd₂(JawsP), and C₆₀ in mole ratio 2:3:4.2, significant shifts can be seen in the peaks of H₄JawsP but not those of Pd₂(JawsP). These data are shown in Figure 6.

Titration of toluene solutions of the three diamagnetic systems (Pd, Zn, and free base) with ¹³C-enriched C₆₀ were followed by ¹³C NMR spectroscopy. The variation of chemical shift allowed calculation of the binding constants, and these are listed in the first three entries of Table 1. The ordering, Pd < Zn < 2H, is consistent with the order of increasing coalescence temperature.

When 2/3 of an equivalent of C₆₀ is added to the copper(II) porphyrin, there is a 2.4 ppm shift upfield in the room-temperature spectrum (Figure S5), not unlike (but somewhat less than) that seen in diamagnetic metalloporphyrins or the free-base porphyrin. This can be understood in terms of the singly occupied d_{x²−y²} orbital of Cu(II) which directs the unpaired spin toward the porphyrinato N atoms rather than toward the fullerene. The resulting anisotropy in the magnetic susceptibility, as reflected in the EPR *g* values for Cu(II)TPP, is small.⁵⁰ Estimates of the pseudocontact or dipolar shift due to this anisotropy,⁵¹ based on X-ray structures of porphyrin fullerene conjugates, suggest a maximum average downfield shift of ca. 0.9 ppm. Combined with the upfield shift due to the porphyrin ring current (ca. 3.2 ppm), the reduced total shift of ca. 2.4 ppm is readily rationalized. The coalescence temperature for the copper system (ca. −45 °C) is slightly higher than those of Pd, Zn, and free base suggesting similar binding strength. This is borne out by detailed fitting of the NMR data which leads to the fourth entry in Table 1.

Although significantly broadened by the presence of unpaired spin, each of the other paramagnetic porphyrin systems investigated [M = Co(II), Mn(II), and Fe(II)] shows phenomenologi-

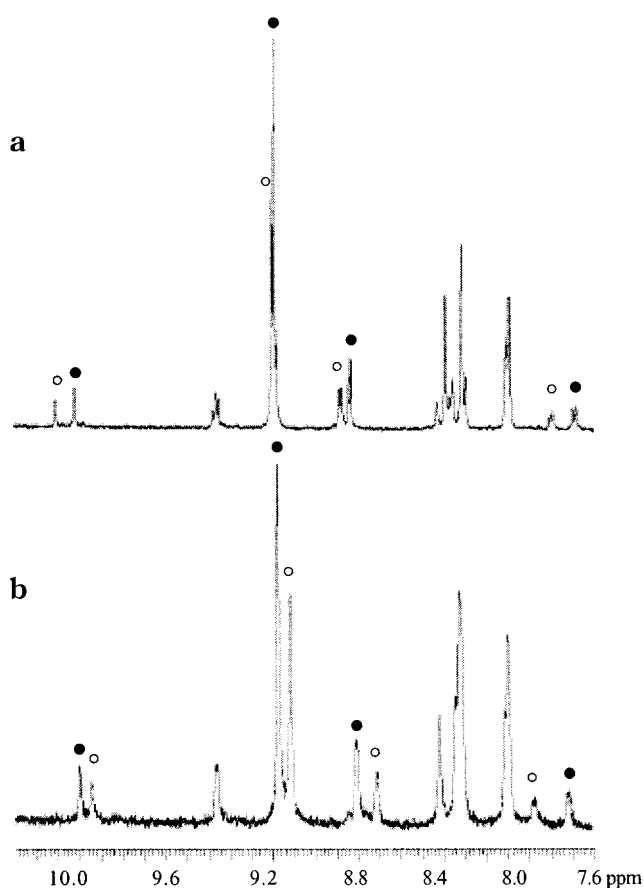


Figure 6. ¹H NMR spectrum of (a) a 2:3 mixture of H₄JawsP (○) and Pd₂(JawsP) (●) with no C₆₀ present and (b) upon addition of an overall stoichiometric deficit of C₆₀ in ratio 2:3:4.2. Peaks due to H₄JawsP, marked with ○, change their chemical shift significantly between (a) and (b).

cally similar variable temperature ¹³C NMR spectra. Extraction of low-temperature limits and relative binding constant data is made more difficult by the overlay of significant intrinsic changes of the chemical shifts as a function of temperature arising from paramagnetism. The spectra for Co₂(JawsP)·C₆₀ are illustrative of the data. Figure 7a shows data with a stoichiometric deficit of C₆₀ to obtain the chemical shift of the complex in the slow exchange regime. At −90 °C, this peak is observed at 192 ppm. Figure 7b shows data with a 2:3 stoichiometric excess of C₆₀ to cleanly observe the coalescence phenomenon, which occurs at 25 °C. Data for the Mn and Fe systems are available as Figures S6 and S7, and a summary is provided in Table 1.

For each of the Mn, Fe, and Co systems, the ¹³C chemical shifts relative to free C₆₀ are downfield. This is an expected result in paramagnetic systems with axial symmetry if the axial magnetic susceptibility is less than the component perpendicular to the principal axis. For Fe(II) and Co(II) porphyrins, this is known to be the case.^{52,53}

Affinity Considerations. The affinity of M₂(JawsP) for C₆₀ increases in the order Fe(II) < Pd(II) < Zn(II) < Mn(II) < Co(II) < Cu(II) < 2H. Studies on a related cyclic bis-porphyrin system⁴¹ show Ag(I) < Ni(II) < Cu(II) < Zn(II) < free base < Co(II) ≪ Rh(III) for C₆₀. There are differences in the ordering

(49) Johnson, R. D.; Bethune, D. S.; Yannoni, C. S. *Acc. Chem. Res.* **1992**, 25, 169–175.

(50) Manoharan, P. T.; Rogers, M. T. *Electron Spin Resonance of Metal Complexes*; Plenum: New York, 1969; pp 143–173.

(51) Horrocks, W. D. In *NMR of Paramagnetic Molecules: Principles and Applications*; La Mar, G. N., Horrocks, W. D., Holm, R. H., Eds.; Academic Press: New York, 1973; Chapter 4.

(52) Goff, H.; La Mar, G. N.; Reed, C. A. *J. Am. Chem. Soc.* **1977**, 99, 3641.

(53) La Mar, G. N.; Fulton, G. P. *J. Am. Chem. Soc.* **1976**, 98, 2119–2123.

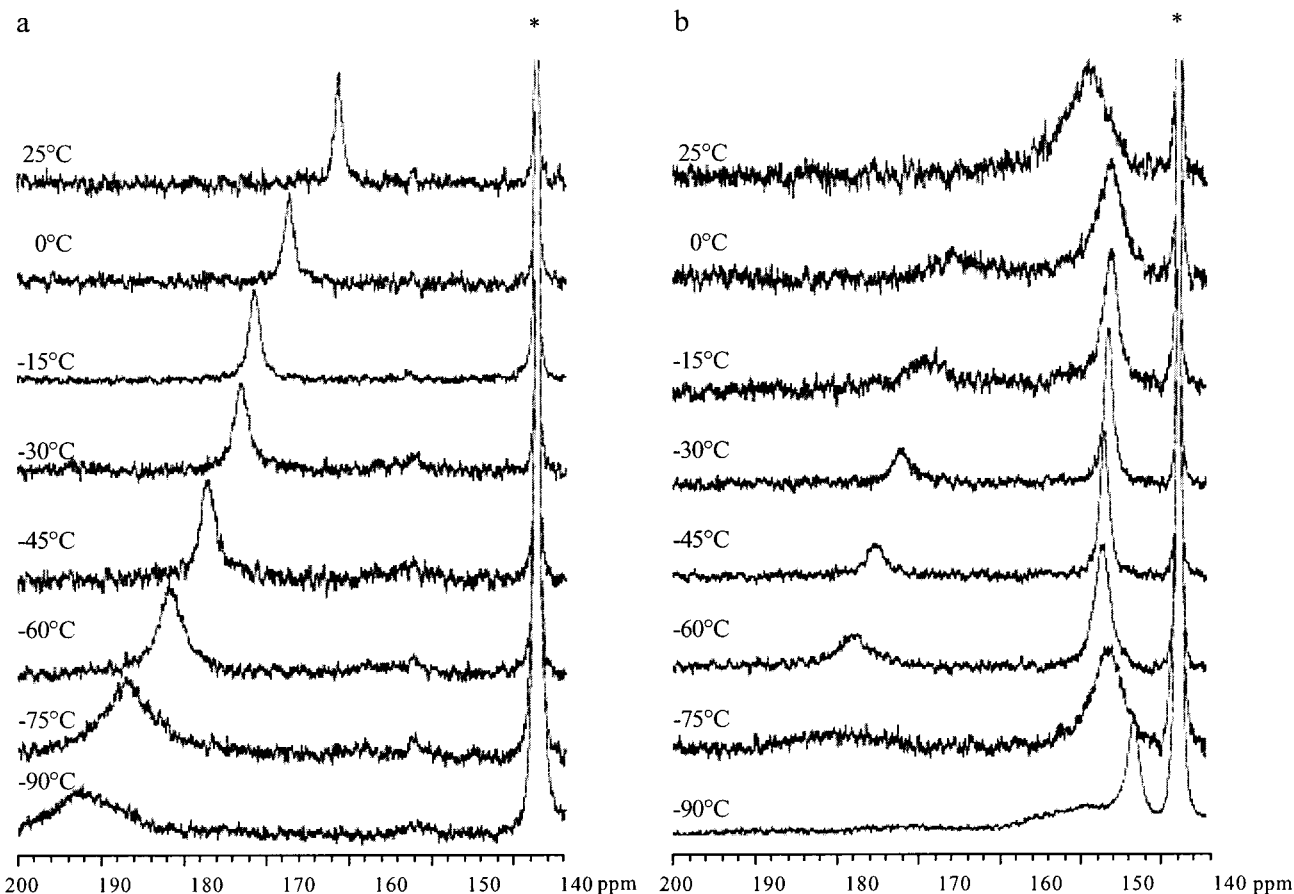


Figure 7. Variable temperature ^{13}C NMR spectra of $\text{Co}_2(\text{JawsP})$ and C_{60} at (a) 2:1 mole ratio and (b) 2:3 mole ratio.

between these two studies, but overall the variation of binding constants as a function of metal is relatively small. Omitting $\text{Rh}(\text{III})$, they vary by less than 900 M^{-1} .

Theory suggests that the attraction of fullerenes to porphyrins and metalloporphyrins is largely van der Waals in nature.⁸ In addition to these dispersion forces, the attraction must also be subject to the subtle interplay of small effects from differences in solvation, electrostatics, charge transfer, and coordinate bond formation.

Interestingly, the free-base porphyrins bind C_{60} somewhat more strongly than most metalloporphyrins. We ascribe this to an electrostatic attraction of the electron-rich 6:6 ring-juncture bond of the fullerene to the electropositive N–H center of the porphyrin. This highlights the importance of an electrostatic component augmenting the π – π host–guest interaction. It is consistent with the observation of stronger binding of endohedral fullerenes and the orientation of the fulleropyrrolidine discussed above.

In the absence of a coordinate interaction, the greater number of electrons associated with metals relative to H atoms leads to the expectation of *stronger* van der Waals interactions with metalated porphyrins relative to free-base porphyrins. However, the data largely confound this expectation. This means that coordinate bonding and dispersion forces due to the metal are rather weak, and less than the electrostatic component present in the free-base interaction. One qualifying consideration is that the van der Waals attraction should not be considered constant throughout the series of metalloporphyrins. Differing degrees of porphyrin ruffling will lead to varying contact areas with

fullerenes, thereby altering the magnitude of the van der Waals component to the binding energy.

It has been suggested that the 2.7–3.0 Å approach of fullerenes to metalloporphyrins is too distant for covalent bonding.^{18,20} This is based primarily on the observation that metal–fullerene distances are “too long for covalence” and the metals are typically not drawn out of their porphyrin planes toward the fullerenes. However, length is a rather subjective criterion of bonding, and metal out-of-plane displacements with weak axial ligands are manifest clearly only in discrete five-coordinate complexes. The presence of face-to-face porphyrin dimers in many X-ray structures effectively adds a competing interaction in the sixth “vacant” coordination site.⁴⁴ Under these circumstances, correlations of axial ligand binding strength often fail to correlate with out-of-plane displacements,¹⁹ and, for weak ligands such as fullerenes and arenes, displacements may be reduced to the level of structural insignificance. We believe it is necessary to view coordinate bonding as a continuum out to at least 3.0 Å.¹⁹ At these distances, the strength of the bonding is obviously very weak, and its degree of covalence small, but the displacement of $\text{Fe}(\text{III})$ from the porphyrin plane in $\text{Fe}(\text{C}_{60})(\text{TPP})^+$ indicates that in favorable circumstances it can be structurally observable. Small changes in UV–vis spectra, the green color of $\text{Fe}(\text{C}_{60})(\text{TPP})^+$, and the measurable perturbation of the metalloporphyrin EPR spectra in the presence of fullerenes²³ all suggest that some degree of charge transfer from the fullerene to the porphyrin via coordinate bonding can occur in favorable circumstances. The magnitude, however, is small and, in many cases, is not a separable effect.

The report of somewhat stronger binding of C_{60} to Rh(III)⁴¹ (and possibly Ru(II) porphyrins)^{22,54} relative to the other metals investigated to date is readily understood. A second row metal utilizing a formal vacant coordination site, whose low-spin d^6 configuration can profit from ligand field stabilization energy when engaged in covalent bonding, has more opportunity to make a significant axial ligand bond. Low-spin d^6 rhodium(III) may even engage in π back-bonding into the fullerene LUMO, taking bonding elements from each of the otherwise fairly distinct classes of metal–fullerene interactions represented by phosphine complexes such as $Ni(C_{60})(PEt_3)_2$ ³⁸ and the hard metalloporphyrin complexes discussed herein.

The remaining structural question is why most metalloporphyrin interactions occur with the 6:6 ring-juncture bond of C_{60} , while some seem to prefer the 5:6 ring juncture. The 6:6 ring-juncture bond is the shorter, more electron-rich (olefinic) bond, although both have double bond character due to π delocalization and aromaticity. The 5:6 interaction is observed in $M^{II}(OEP) \cdot C_{60}$ ($M = Pd, Cu, Ni$) and $Ru^{II}(CO)(OEP) \cdot C_{60}$, and the presence of π antibonding interactions has been suggested.^{20,22} If coordinate bonding is involved, we expect the 6:6 interaction to be preferred because it can better provide σ donation to the metal. However, in the Pd, Cu, and Ni structures, the $M \cdots C$ distances are all very long (2.99–3.07 Å), correlating with the low affinities. The 5:6 orientations may simply reflect a lack of significant preference and control by crystal packing interactions whose influences are difficult to assess. Particular conformations of the ethyl substituents in these three compounds have been noted.^{20,22} The 5:6 orientation with shorter metal–carbon distances in the ruthenium(II) case (2.83–2.86 Å)²² is more difficult to rationalize. However, packing effects from the ethyl groups of the OEP may again be a factor. More data are needed to learn whether there is generality to this observation.

The report that the order of binding constants changes slightly between C_{60} and C_{70} ⁴¹ shows that subtle differences in solvation energies are another factor affecting affinities.

Overall, it is clear that a number of small effects conspire to affect binding constants in ways that do not always lend themselves to easy deconvolution. Depending on the physical property that is measured, the effect may or may not be detectable. A continuum of weak bonding forces from coordinate bonding to dispersion forces, that is, from weak ligation to solvation,¹⁹ is preferable to arbitrary limits or categorical statements about presence or absence.

Conclusions

The identification of an attractive fullerene–porphyrin interaction represents a new supramolecular recognition element. It can be fine-tuned with metals in the porphyrins through a subtle interplay of coordinate bonding, charge transfer, electrostatics, and solvation energy effects. It differs from traditional π – π interactions by the closeness of the approach and the surprising affinity of a curved molecular surface to a planar surface. This offers new opportunities to assemble discrete supramolecular complexes as well as extended solids. We anticipate that the molecular design principles emanating from these studies will be most useful in the manipulation of photophysical properties, adjusting charge transfer in molecular

magnets and molecular conductors, and in the creation of new porous metal-organic frameworks.¹⁶

Experimental Section

General. All manipulations involving air-sensitive materials were performed in a Vacuum Atmospheres glovebox (O_2 , H_2O , 0.5 ppm). Toluene and THF were dried by distillation from Na/benzophenone outside the glovebox and again inside the box prior to use. Toluene- d_8 was dried over molecular sieves and filtered through a 0.2 μ syringe filter prior to use. “Jones reductor” Zn(Hg) was prepared by treating Zn pellets with dilute $HgCl_2$ solution, washing with dilute hydrochloric acid then water, and drying under vacuum. ^{13}C -enriched C_{60} (10–15%) was purchased from MER Corp. Meso-3-pyridyl-triphenylporphyrin and the $PdCl_2$ -linked dimer, H_4JawsP , were prepared as previously described.³⁰ $C_{120}O$ ^{55,56} and *N*-methylpyrrolidine-derivatized C_{60} ⁵⁷ were prepared by literature methods. Host–guest complexes were prepared by additions of fullerenes and porphyrins in toluene. NMR spectra were recorded in toluene- d_8 on an Inova 500 MHz spectrometer and internally referenced to residual protio peaks of the solvent. MALDI TOF mass spectra were recorded on a PerSeptive Biosystems Voyager-DE STR instrument operated in linear mode with laser intensity of ca. 2000 eV. Air-stable samples were mixed with dithronol matrix. Air-sensitive samples were used directly, loading under anaerobic conditions. Titrations were performed with 10^{-3} M solutions of porphyrins and incremental additions of 10^{-3} M solutions of ^{13}C -enriched C_{60} dissolved in the porphyrin stock solution. Binding constants were determined from the variation in ^{13}C NMR shifts using the WinEQNMR program.⁵⁸

Molecular Modeling. Host/guest complexes were constructed using the program CERIUS2.⁵⁹ Geometry optimization was carried out using the universal force field.⁶⁰ Gas-phase binding energies were estimated by comparison of the energy of the porphyrin–fullerene complex with the optimized energies of C_{60} and the bis-porphyrin. In this model, the gas-phase interaction energy of a single porphyrin with C_{60} is between 28 and 30 kcal mol^{−1} depending on the porphyrin substituents. Bis-porphyrins that give effective fullerene binding are found to have about twice this energy, while those with weaker binding are less. The main feature contributing to weaker binding is the strain imposed on some hosts upon complexation. Semiempirical MO calculations using the PM3 method⁴⁵ were carried out using SPARTAN (Version 5.1, Wave function Inc.). A Mulliken population analysis was performed on the PM3 optimized structure to estimate the atomic charge distribution on the fullerene.

H_4JawsP'' and H_4JawsP' . These were prepared by slow addition of 100 mg of 5-(3-aminophenyl)10,15,20-(*p*-methylphenyl)porphyrin⁶¹ dissolved in 5 mL of dichloromethane containing triethylamine to a 5 mL solution containing 14.2 mg of either 1,4- or 1,3-di(chlorocarbonyl)-benzene. The mixture was stirred under a nitrogen atmosphere for 24 h at room temperature. The product was precipitated by addition of hexane and purified by chromatography on a silica gel column using dichloromethane and dichloromethane/ether (9.8:0.2) eluents. Both products gave parent ions in FAB mass spectra using *m*-nitrobenzyl alcohol as a matrix: H_4Jaws'' m/z 1473.6 [M^+ 1473.6, $C_{102}H_{76}N_{10}O_2$]; H_4Jaws' m/z 1473.616 (accurate mass) [M^+ 1473.618, $C_{102}H_{76}N_{10}O_2$].

$Pd_2(JawsP)$. Meso-3-pyridyl-triphenylporphyrin was heated with a large excess of $PdCl_2(DMSO)_2$ in toluene for ca. 4 h or in $CHCl_3$ for

(54) Maruyama, H.; Fujiwara, M.; Tanaka, K. *Chem. Lett.* **1998**, 805–806.

- (55) Lebedkin, S.; Ballenweg, S.; Gross, J.; Taylor, R.; Krätschmer, W. *Tetrahedron Lett.* **1995**, 36, 4971–4974.
 (56) Taylor, R.; Barrow, M. P.; Drewello, T. *J. Chem. Soc., Chem. Commun.* **1998**, 2497–2498.
 (57) Drovetskaya, T.; Reed, C. A.; Boyd, P. D. W. *Tetrahedron Lett.* **1995**, 36, 7971–7974.
 (58) Hynes, M. J. *J. Chem. Soc., Dalton Trans.* **1993**, 311–331.
 (59) CERIUS2; Molecular Simulations: San Diego, CA, 1997; Version 3.5.
 (60) Rappe, A. K.; Casewit, C. J.; Colwell, K. S.; Goddard, W. A.; Skiff, W. M. *J. Am. Chem. Soc.* **1992**, 114, 10024–10035.
 (61) Liddell, P. A.; Sumida, J. P.; MacPherson, A. N.; Noss, L.; Seely, G. R.; Clark, K. N.; Moore, A. L.; Moore, T. A.; Gust, D. *Photochem. Photobiol.* **1994**, 60, 537.

ca. 2 days to accomplish Pd pyridyl linking and porphyrin metalation in one step. Completion of reaction was checked by ^1H NMR via loss of the pyrrole N–H resonance at -2.14 ppm, and the product was purified by flash chromatography on silica gel with chloroform as eluent. m/z 2292 $[\text{M} + \text{H}]$ plus monomer fragment at 1055. See Figure S8 for simulation of isotopes. ^1H NMR: 9.81 (1H, s, pyridyl), 9.16 (1H, d, pyridyl), 8.94 (6H, m, phenyl), 8.65 (3H, d, phenyl), 8.06 (6H, m, pyrrole), 7.83 (2H, m, pyrrole), 7.69 (1H, t, pyridyl), 6.78 (1H, t, pyridyl), 1.34 and 0.91 (54H, m, t-Bu) ppm. UV–vis (toluene): 422 (Soret), 526, 602 nm.

$\text{Cu}_2(\text{JawsP})$. H_4JawsP in CHCl_3 was treated 2 equiv of $\text{Cu}(\text{OAc})_2$ dissolved in minimum methanol under reflux for 2 h. Purification was achieved by column chromatography on silica gel with dichloromethane as eluent. m/z 2206 $[\text{M} + \text{H}]$; free base was absent. ^1H NMR (broad): 9.18, 7.82, 7.58, 6.43, 1.34 ppm. UV–vis (toluene): 421 (Soret), 541, 580 nm.

$\text{Co}_2(\text{JawsP})$. This was prepared in a manner similar to $\text{Cu}_2(\text{JawsP})$ using $\text{Co}(\text{OAc})_2$. m/z 2195 $[\text{M}^+]$; free base was absent. ^1H NMR (broad): 11.70, 9.86, 9.09, 1.33, 0.92. UV–vis (toluene): 420 (Soret), 526, 606, 655 nm.

$\text{Zn}_2(\text{JawsP})$. This was prepared in a manner similar to $\text{Cu}_2(\text{JawsP})$ using $\text{Zn}(\text{OAc})_2$. m/z 2211 $[\text{M} + \text{H}]$; free base was absent. ^1H NMR: 10.18 (1H, pyridyl), 9.32 (1H, pyridyl), 9.17, 9.13 (6H, phenyl), 8.99, 8.81 (3H, phenyl), 8.34, 8.29, 7.94 (8H, pyrrole), 8.13 (1H, pyridyl), 6.78 (1H, pyridyl), 1.49 and 0.92 (54H, t-Bu) ppm. UV–vis (toluene): 426 (Soret), 552, 592 nm.

$\text{Mn}_2(\text{JawsP})$. This was prepared under anaerobic conditions by treatment of H_4Jaws with an equal weight of MnBr_2 in toluene/THF under reflux in the presence of K_2CO_3 for 2 days. After filtration, the product was purified by recrystallization from toluene/THF. UV–vis (toluene): 429 (Soret), 452, 595, 638 nm. m/z (no matrix) 1004 $[\text{M}^+ \text{ for monomeric Mn porphyrin}]$; free base was absent.

$\text{Fe}_2(\text{JawsP})$. This was prepared in a manner similar to $\text{Mn}_2(\text{JawsP})$ using FeBr_2 . Stirring with product solution over $\text{Zn}(\text{Hg})$ pellets removed traces of $\text{Fe}(\text{III})$ porphyrin. UV–vis (toluene): 432 (Soret), 455, 545 nm. m/z (no matrix) 1006 $[\text{M}^+ \text{ for monomeric Fe porphyrin}]$; free base was absent.

X-ray Structure Determinations. **$\text{Cu}_2(\text{JawsP}) \cdot \text{C}_{60} \cdot 1.5\text{hexane}$.** Black crystals were grown by layered diffusion of hexanes into a toluene solution of 1:1 $\text{Cu}_2(\text{JawsP})$ and C_{60} . A fragment of a thin needle ($0.27 \times 0.21 \times 0.04 \text{ mm}^3$) was used. The crystal was mounted onto a glass fiber and coated with epoxy resin to prevent the loss of solvent of crystallization. X-ray intensity data were collected at 213(2) K with the CCD detector placed at a distance of 4.8450 cm from the crystal. On the basis of a orthorhombic crystal system, the integrated frames yielded a total of 93 497 reflections at a maximum 2θ angle of 43.94° (0.95 \AA resolution), of which 10 882 were independent reflections ($R_{\text{int}} = 0.0996$, $R_{\text{sig}} = 0.0722$, redundancy = 8.6, completeness = 100%) and 6566 (60.3%) reflections were greater than $2\sigma(I)$. The unit cell parameters were $a = 27.903(2) \text{ \AA}$, $b = 43.578(3) \text{ \AA}$, $c = 29.242(2) \text{ \AA}$, $\alpha = 90^\circ$, $\beta = 90^\circ$, $\gamma = 90^\circ$, $V = 35\,556(5) \text{ \AA}^3$, $Z = 8$, calculated density $D_c = 1.190 \text{ g/cm}^3$. Absorption corrections were applied (absorption coefficient $\mu = 0.424 \text{ mm}^{-1}$) to the raw intensity data using the SADABS program in the SAINTPLUS software.⁶² The maximum/minimum transmission factors were 0.9833/0.8942. The Bruker SHELXTL (Version 5.1) software package⁶³ was used for phase determination and structure refinement. The distribution of intensities

($E^2 - 1 = 0.936$) and systematic absent reflections indicated one possible space group, *Ccca*. The space group *Ccca* was later determined to be correct. Patterson method was used to locate the Pd and Cu atoms. Subsequent isotropic least-squares refinements led to an electron density map from which all of the non-hydrogen atoms were identified in the asymmetry unit of the unit cell, including the four partially occupied hexane solvent molecules. The site occupancy factors for the four hexane molecules were 50, 47, 36, and 17%, which gave a total of 1.5 hexane molecules in the asymmetry unit. The C_{60} , the four partially occupied hexane molecules, and the nine disordered methyl groups were modeled as rigid groups using the EQIV, SADI, DFIX, DELU, SIMU, ISOR commands. The C_{60} and the Pd1 atom were located on a 2-fold rotation axis ($-x, y, 1.5 - z$ symmetry operator). Atomic coordinates and isotropic and anisotropic displacement parameters of all the non-hydrogen atoms were refined by means of a full matrix least-squares procedure on F^2 . All H-atoms were included in the refinement in calculated positions riding on the atoms to which they were attached. The refinement converged at $R1 = 0.0598$, $wR2 = 0.1638$, with $I > 2\sigma(I)$. The largest peak/hole in the final difference map was $1.088/-0.791 \text{ e/\AA}^3$.

$\text{H}_4(\text{JawsP}) \cdot (N\text{-methylpyrrolidino-C}_{60}) \cdot 0.5\text{hexane}$. Black crystals were grown by layered diffusion of hexanes into a toluene solution of 1:1 2-(*N*-methylpyrrolidino)- C_{60} ⁶⁴ and $\text{Cu}_2(\text{JawsP})$. Details of the structure solution and refinement are given in the Supporting Information. Orthorhombic *Ccca*: $a = 27.585(3) \text{ \AA}$, $b = 43.432(4) \text{ \AA}$, $c = 29.246(3) \text{ \AA}$, $\alpha = 90^\circ$, $\beta = 90^\circ$, $\gamma = 90^\circ$, $V = 35039(6) \text{ \AA}^3$, $Z = 8$, $D_c = 1.115 \text{ g/cm}^3$, $2\theta_{\text{max}} = 46.52^\circ$, 83 188 measured reflections, 12 601 independent reflections, 7734 with $I > 2\sigma(I)$ used for refinement to give $R1 = 0.0624$, $wR2 = 0.1617$.

$\text{H}_4(\text{JawsP}) \cdot 2\text{C}_{70} \cdot 3\text{toluene} \cdot 1.5\text{hexane}$. Black crystals were grown by layered diffusion of hexanes into a 1:1 toluene solution of $\text{H}_4(\text{JawsP})$ and C_{70} . Details of the structure solution and refinement are given in the Supporting Information. $\text{C}_{134}\text{H}_{150}\text{Cl}_2\text{N}_{10}\text{Pd}(\text{C}_{70})_2 \cdot (\text{C}_7\text{H}_8)_3(\text{C}_6\text{H}_{14})_{1.5}$, monoclinic *C2/c*, $a = 39.032(6) \text{ \AA}$, $b = 30.454(5) \text{ \AA}$, $c = 38.496(6) \text{ \AA}$, $\alpha = 90^\circ$, $\beta = 106.912(3)^\circ$, $\gamma = 90^\circ$, $V = 43781(12) \text{ \AA}^3$, $Z = 8$, $D_c = 1.264 \text{ g/cm}^3$, $2\theta_{\text{max}} = 34.46^\circ$, 47 939 measured reflections, 13 269 independent reflections, 6144 with $I > 2\sigma(I)$ used for refinement to give $R1 = 0.1196$, $wR2 = 0.3376$.

Acknowledgment. We thank Dr. Robert Bolskar of TDA for samples of higher and endohedral fullerenes, Prof. Michael J. Hynes for a copy of WinEQNMR, and Drs. Parimal Paul, Daniel Stasko, Alex Clark, Steven Kennedy, Richard Kondrat, Mehrnoosh Sadeghi, and Yi Meng for assistance. This work was supported by the National Institutes of Health (GM 23851) and the Marsden Fund of The Royal Society of New Zealand (00-UOA-030).

Supporting Information Available: MALDI mass spectra (Figures S1–S4 and S8), NMR spectra (Figures S5–S7), and X-ray data (PDF). This material is available free of charge via the Internet at <http://pubs.acs.org>.

JA017555U

(62) SAINTPLUS Software Reference Manu; Bruker Analytical X-ray System, Inc.: Madison, WI, 1997–1998; Version 5.02.

(63) SHELXTL Software Reference Manual; Bruker Analytical X-ray System, Inc.: Madison, WI, 1997–1998; Version 5.1.

(64) Maggini, M.; Scorrano, G.; Prato, M. *J. Am. Chem. Soc.* **1993**, *115*, 9798–9799.